

CONF-890231-6

ANL-HEP-CP--89-33

DE89 013276

THE SOUDAN 2 PROTON DECAY EXPERIMENT

Jonathan L. Thron

Argonne National Laboratory

for the Argonne, Minnesota, Oxford, Rutherford, Tufts Collaboration

JUN 02 1989

1 INTRODUCTION

The Soudan 2 proton decay experiment is now 1/4 complete and assembled at the bottom of the Soudan iron mine in northern Minnesota, USA. When completed, it will be an 1100 ton, fine grained, iron calorimeter. It is comprised of 256 identical modules. The cavity is $14 \times 72 \times 11$ m (w \times l \times h) large enough to accommodate a 3300 ton detector of similar design.

The detector samples track positions every 15, 10, and 2mm along the three spatial coordinates. Thus, the detector will have excellent tracking capabilities for the low energy charged particles and electromagnetic showers expected from nucleon decay candidates and neutrino background events. In addition, for such events the energy of particles observed is sufficiently low that they will stop inside the detector. The measurement of the ionization deposited as a function of track length allows the determination of track direction and will yield some information on the particle type.

In addition to the dE/dx measurements the Soudan 2 detector has several advantages over previous nucleon decay detectors. The honeycomb geometry has very isotropic detection compared with other tracking detectors. The thin steel and local triggering system produces a low trigger threshold giving excellent efficiency for multiparticle decay modes or ones with missing energy due to neutrinos.

2 THE DETECTOR

The basic detection element of the experiment is shown in Fig. 1. It is a resistive ($\sim 4 \times 10^{12} \Omega$ -cm) plastic (Hytrel) tube, one meter long with an inner diameter of 15mm and a thickness of .5 mm. A graded electric field is applied along it by 21, 1.5 mm wide copper electrodes. These have a voltage of -9 KV at the middle of the tube and 0 V at the two ends. The resistive tube then grades the voltage between electrodes, creating a uniform axial drift field of 180 V/cm inside the tube. The tubes are filled with a pure gas of 85% argon, 15% CO_2 and a few tenths of a percent H_2O . When a charged particle passes through the tube it ionizes the gas; the liberated electrons then drift (with a velocity of .6 cm/ μ sec) up to 50 cm to the ends of the tube where they are collected and amplified on a 50 μ m diameter anode wire (gold plated tungsten).

The tubes are arranged in an hexagonally close packed array as shown in Fig. 2. The anode wires run vertically in a plane 10 mm from the tube ends and are spaced every 15 mm so that they are aligned with the centers of the tubes. Cathode pads are connected in horizontal strips orthogonal to the anode wires 5 mm behind them, and are aligned with the tubes. Thus it is possible to identify which tube a signal came from since the anodes and the cathodes provide a two coordinate grid centered on the tube ends.

Work supported by the U.S. Department of Energy, Division of High Energy Physics, Contract W-31-109-ENG-38.

DISTRIBUTION OF THIS DOCUMENT IS UNLIMITED

MASTER

Most of the mass of the detector is provided by 1.6 mm thick steel sheets which are corrugated so as to hold the tubes in position. They are 1 m \times 1 m after corrugating. In order for the drift high voltage to make contact with the tubes and still keep them insulated from the steel sheets, the tubes are sandwiched between two sheets of mylar 1 m wide and 125 μ m thick (see Fig. 3). The copper strip electrodes are laminated onto the inside of the mylar where they provide high voltage to the tubes but are insulated from the steel.

The steel sheets and the assembly of tubes, copper, and mylar (called a 'bandolier') are then stacked up for 240 layers (2.5 m) to form 4.2 ton modules. In doing this the bandolier is fanfolded back and forth with steel sheets interleaved. For additional insulation, a .5 mm thick sheet of polystyrene is placed on both sides of each sheet of steel in the stack. The polystyrene is vacuum formed to conform to the shape of the steel. These stacks are then compressed with 15 tons of force to achieve a uniform module height. A steel skin is then welded around 4 faces of the module. This skin keeps the stack compressed and provides the gas seal on those sides. The other two faces of the module are where the readout planes are mounted. The planes must be flat and rigid in order to maintain a constant wire gain across the many tubes. This is done with an aluminum/G-10 frame holding the wires. The cathodes are etched copper on G-10 with a Hexcel/G-10 sandwich backing and are also attached to the frame.

The modules are then assembled into the full underground detector by stacking them together 2 high by 8 across by 16 long. The relatively small module size was chosen so that they could be built on the surface and still carried down the mine shaft. Additionally, since they are self contained gas volumes, they can be used to test sections of the actual detector in neutrino and charged particle beams.

The Soudan 2 detector is read out by 16128 anode wires and 30720 cathode strips. Signals from preamps on each wire or strip are bussed together in groups of 8 to reduce the number of ADC channels. The resulting 5888 channels of ionization signal are digitized by flash ADC's every 200 ns and stored in RAM. This provides both a pulse height profile of the signals and measures the drift time down a tube, thereby giving the z coordinate of a hit.

The raw data hit patterns are continually compared with programmable trigger conditions. This gives a very flexible trigger, due to its adjustable parameters. Since every readout channel is involved in the trigger process the trigger is uniform throughout the detector volume. The trigger system has $> 80\%$ efficiency for muons with total energy down to 250 MeV, while accepting less than 0.5 Hz of random triggers due to natural radioactivity.

3 PERFORMANCE RESULTS

The cosmic ray test stand is above ground, where there are many more cosmic rays. It holds one module and provides a scintillator trigger with a counter above the module and one below the 15 cm thick steel base of the stand. In order to satisfy the trigger the cosmic rays must be energetic enough to go through the module and the base slab. The cosmic rays are mostly vertical and illuminate the whole volume of the module fairly uniformly.

The cosmic ray tracks are useful for measuring pulse height and efficiency uniformity through out the detector volume. Figure 4a shows the anode-drift time view of a cosmic ray track while Fig. 4b shows the cathode-drift time view. The bottom scale is in 200 ns clock counts. For the individual pulses the microstructure of each 200 ns pulse height sampling can barely be seen. Since a cloud of electrons drifting down a tube to an anode wire will produce a signal on the anode wire and simultaneously on some cathode, it is possible to reconstruct which individual tube a signal came from. Additional matching information comes from looking at the pulse heights (the cathode will be a known fraction of the anode signal) and the pulse shapes. Thus for each tube crossing of a charged particle all three position coordinates are measured as well as the pulse height. Figure 4c shows the reconstructed anode-cathode view of the track.

The data are analyzed using a track fitting program. Figure 5 shows the rms residuals of the data from the fitted line for the coordinate along the drift direction. From the mean value one can tell that the tube to tube drift velocity variation is less than 1%. The mean is expected to be reduced in later analyses by determining the position of a pulse not just by the leading edge, but by taking into account the pulse shape, the time to get above threshold and the longitudinal diffusion during drifting.

In drifting electrons for 50 cm it is important to know the amount of attenuation which occurs. Figure 6 shows a plot of pulse height versus drift distance (from 10 to 45 cm). The superposed line is a fit to an exponential fall off and gives an attenuation length of 124 ± 5 cm. This is to be compared to the maximum value obtainable, due only to diffusion into the tube walls, of 135 cm.

In addition to through-going cosmic ray tracks, the module performance is studied by looking at Fe^{55} sources which were temporarily placed in the module during its construction. Since the Fe^{55} sources provide a known amount of ionization, they are used to study the effects of different amounts of gas impurities, different anode wire voltages and the pulse height resolution of the system. Also, since they are at a known location they are used to see gas gain variations and measure the attenuation process for the drifting electrons. From these sources a 10% energy resolution is measured, well within the over all detector design goal of 20%, although the resolution will be degraded due to wire to wire gain variations and for less predictable sources of ionization (e.g. cosmic rays).

To check the dE/dx capability of the detector, the scintillator trigger on the cosmic ray test stand was reconfigured to pick out tracks which entered but didn't leave the module. These events were scanned to throw out showers, accidentals, etc. The remainder were a clean sample of stopping muons. Starting with the muon end point and working back up the track, the dE/dx vs distance left to go was obtained. Figure 7 shows this plot for 300 events. The superposed curve is the Bethe-Bloch equation for the material in the detector.

For individual stopping tracks, the track direction can be determined by comparing the ionization at the end of the track with that at some point on the track where it is closer to minimum ionizing. Figure 8 shows that for the stopping muon sample (all of which came in from above) the track direction is

correctly determined 86% of the time by comparing the average pulse height in the last 5cm with that in the 5 cm region 20 cm further up the track. Track direction determination is important for distinguishing proton decays from neutrino backgrounds.

Work supported by the U.S. Department of Energy, Division of High Energy Physics under Contract W-31-109-ENG-38 and the Science and Engineering Research Council, United Kingdom.

DISCLAIMER

This report was prepared as an account of work sponsored by an agency of the United States Government. Neither the United States Government nor any agency thereof, nor any of their employees, makes any warranty, express or implied, or assumes any legal liability or responsibility for the accuracy, completeness, or usefulness of any information, apparatus, product, or process disclosed, or represents that its use would not infringe privately owned rights. Reference herein to any specific commercial product, process, or service by trade name, trademark, manufacturer, or otherwise does not necessarily constitute or imply its endorsement, recommendation, or favoring by the United States Government or any agency thereof. The views and opinions of authors expressed herein do not necessarily state or reflect those of the United States Government or any agency thereof.

Cut away of the Basic Drift Tube Operation

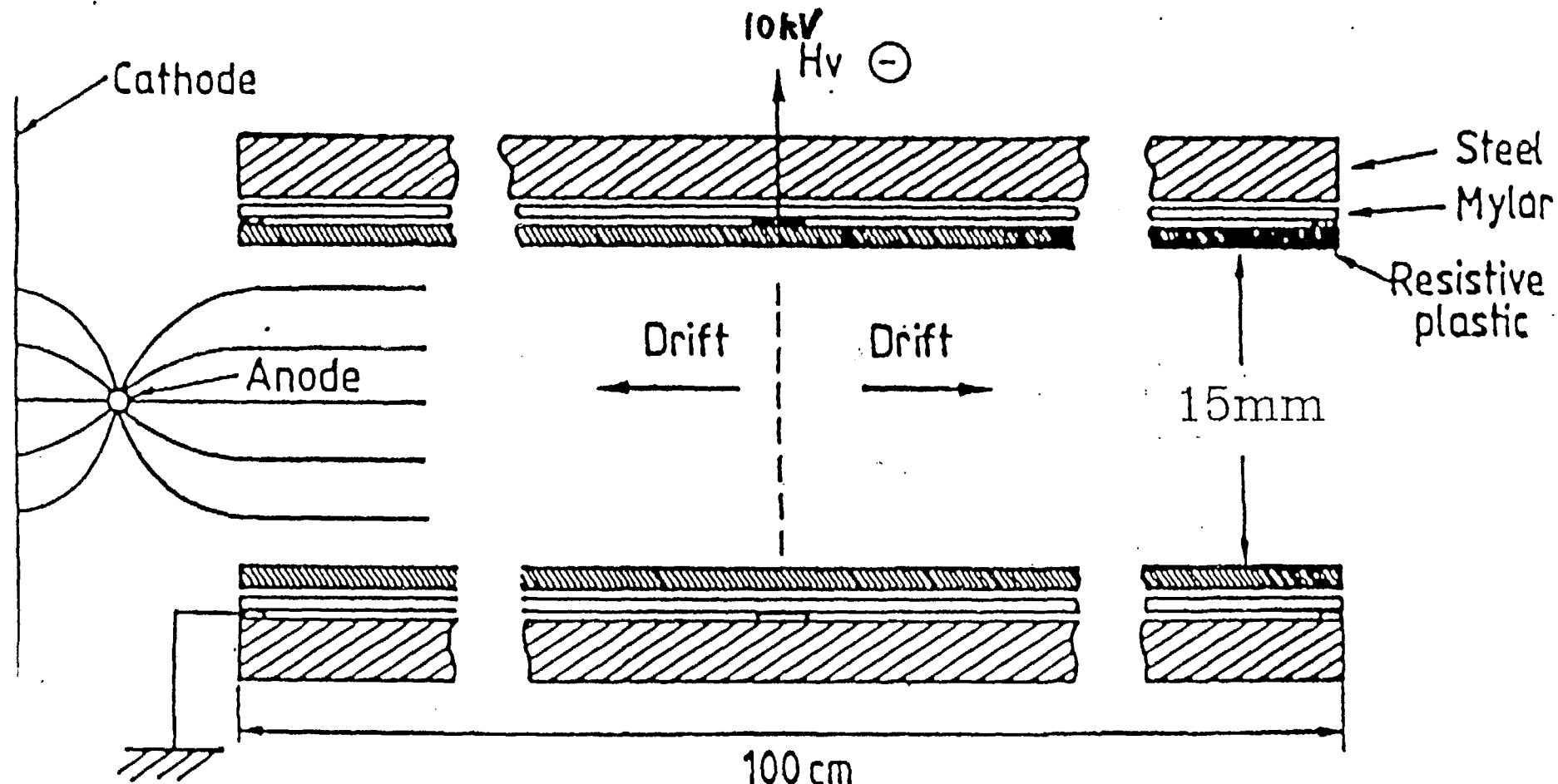


Fig. 1. A longitudinal section of the basic 1m resistive plastic drift tube showing the the surrounding mylar insulation and the steel sheets.

End View of the Drift Tubes

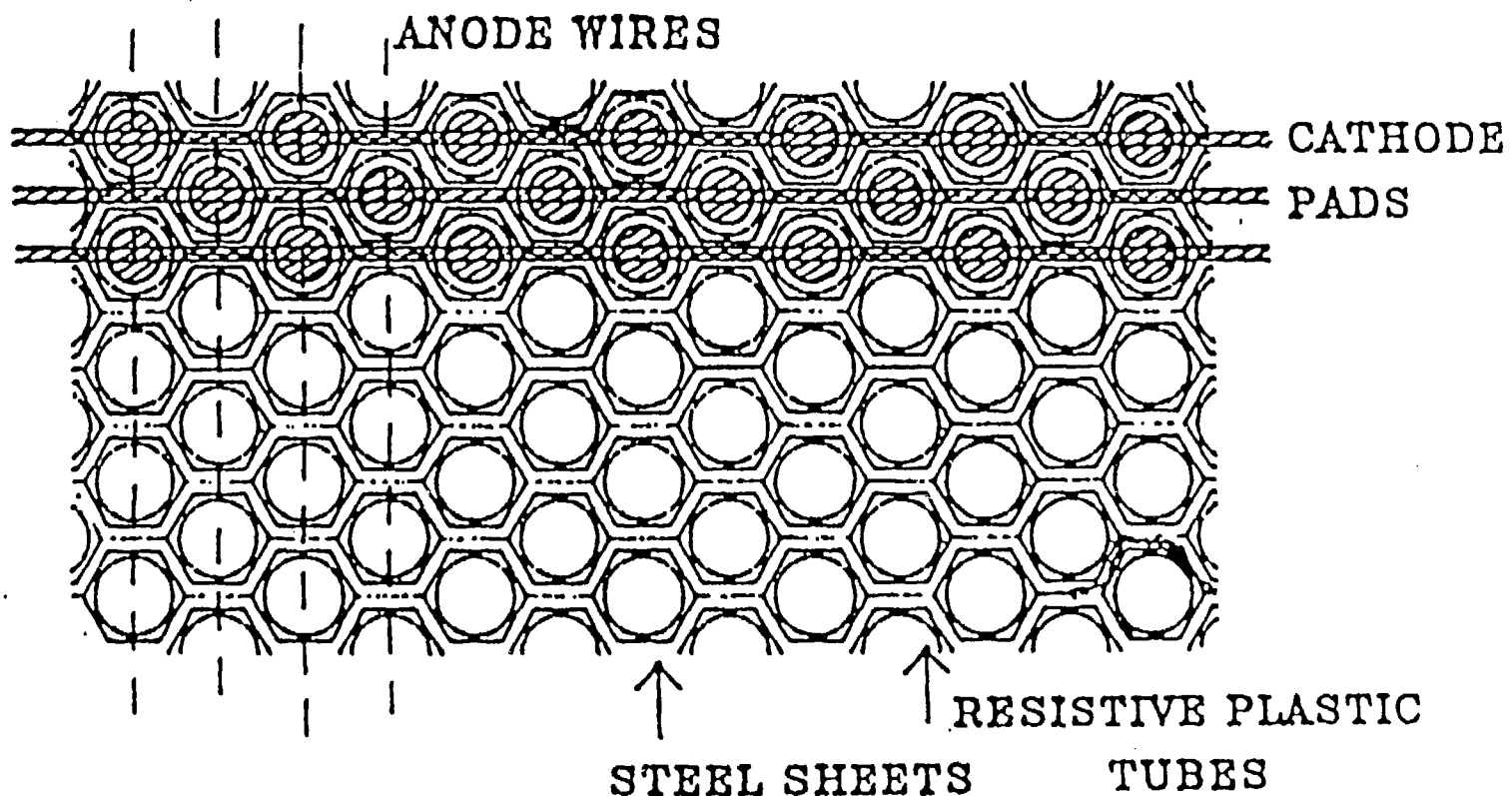


Fig. 2. An end-on view of the hexagonally close packed drift tubes and the steel sheets. The readout by orthogonal anode wires and cathode strips is shown.

Fig. 3. A section of the 'bandolier' showing the drift tubes bonded between two layers of mylar with the copper equipotentials.

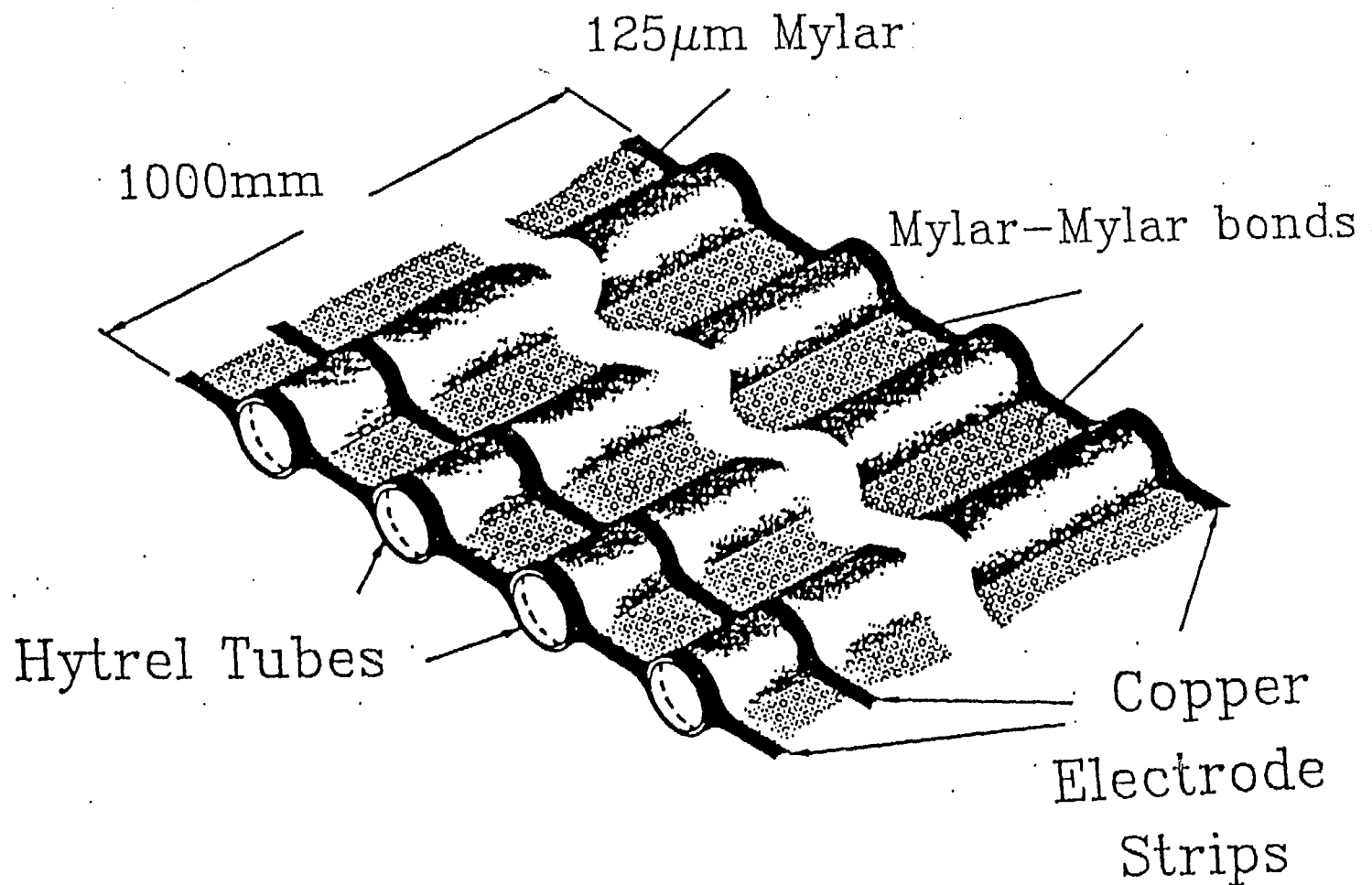


Fig. 4a. A anode number - drift time view of a cosmic ray track in a module.

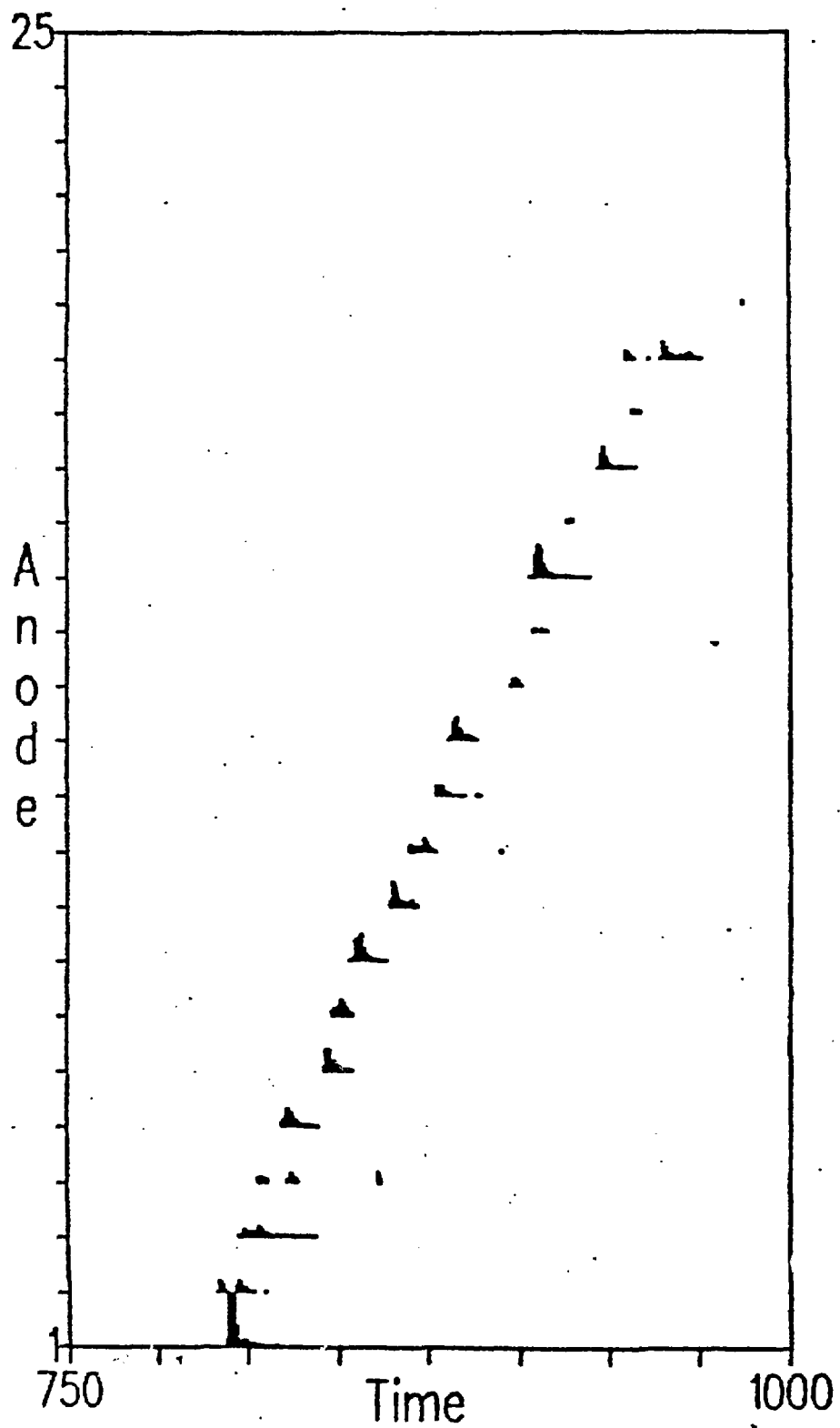


Fig. 4b. A cathode number - drift time view of a cosmic ray track in a module.

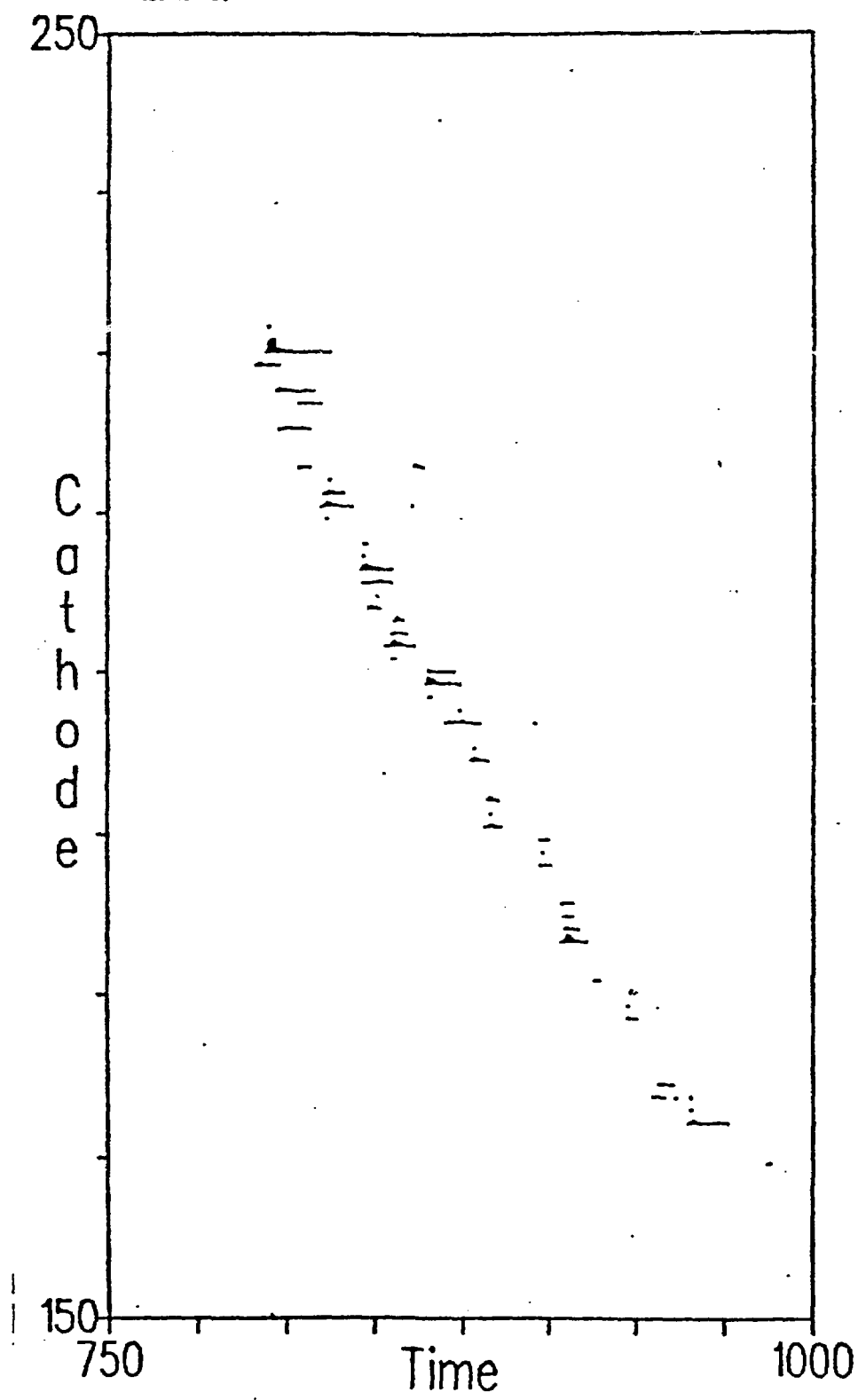
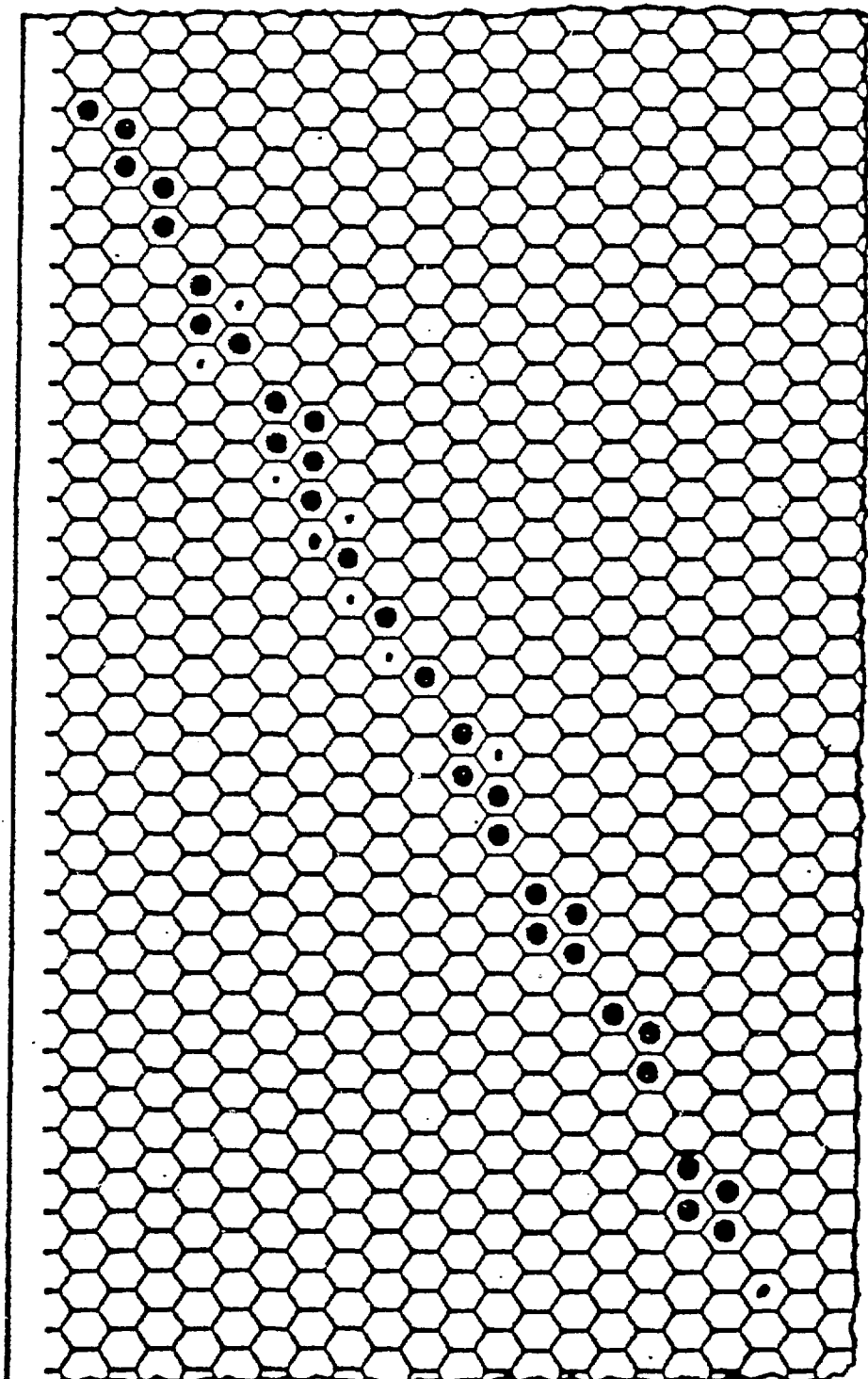
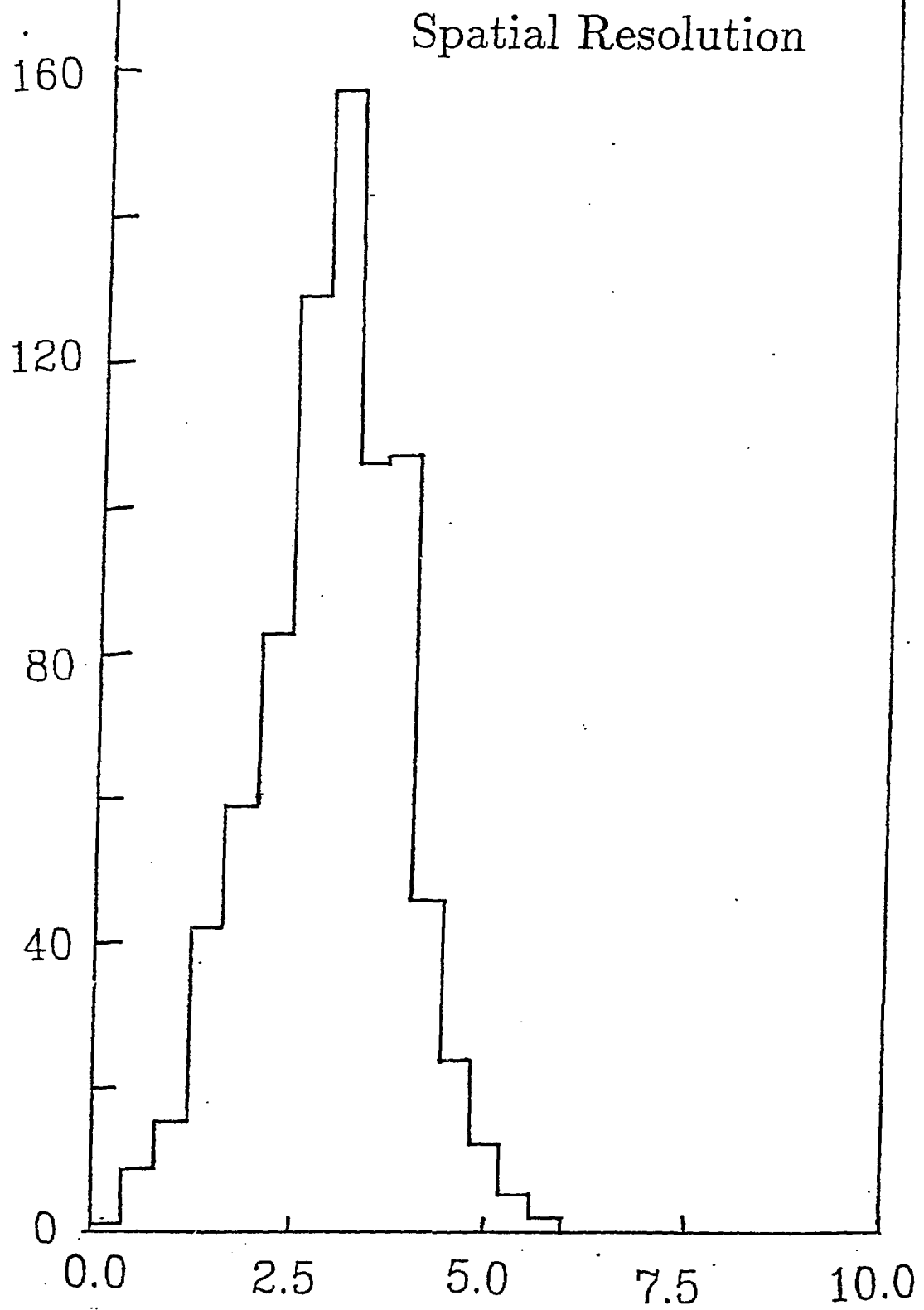


Fig. 4c. The reconstructed anode - cathode view of the cosmic ray track.



← ANODES →

Fig. 5. The rms residual of cosmic ray track data from the fitted lines in the drift distance dimension.



RMS Residual in Drift Direction (mm)

Pulse Height Attenuation with Drifting

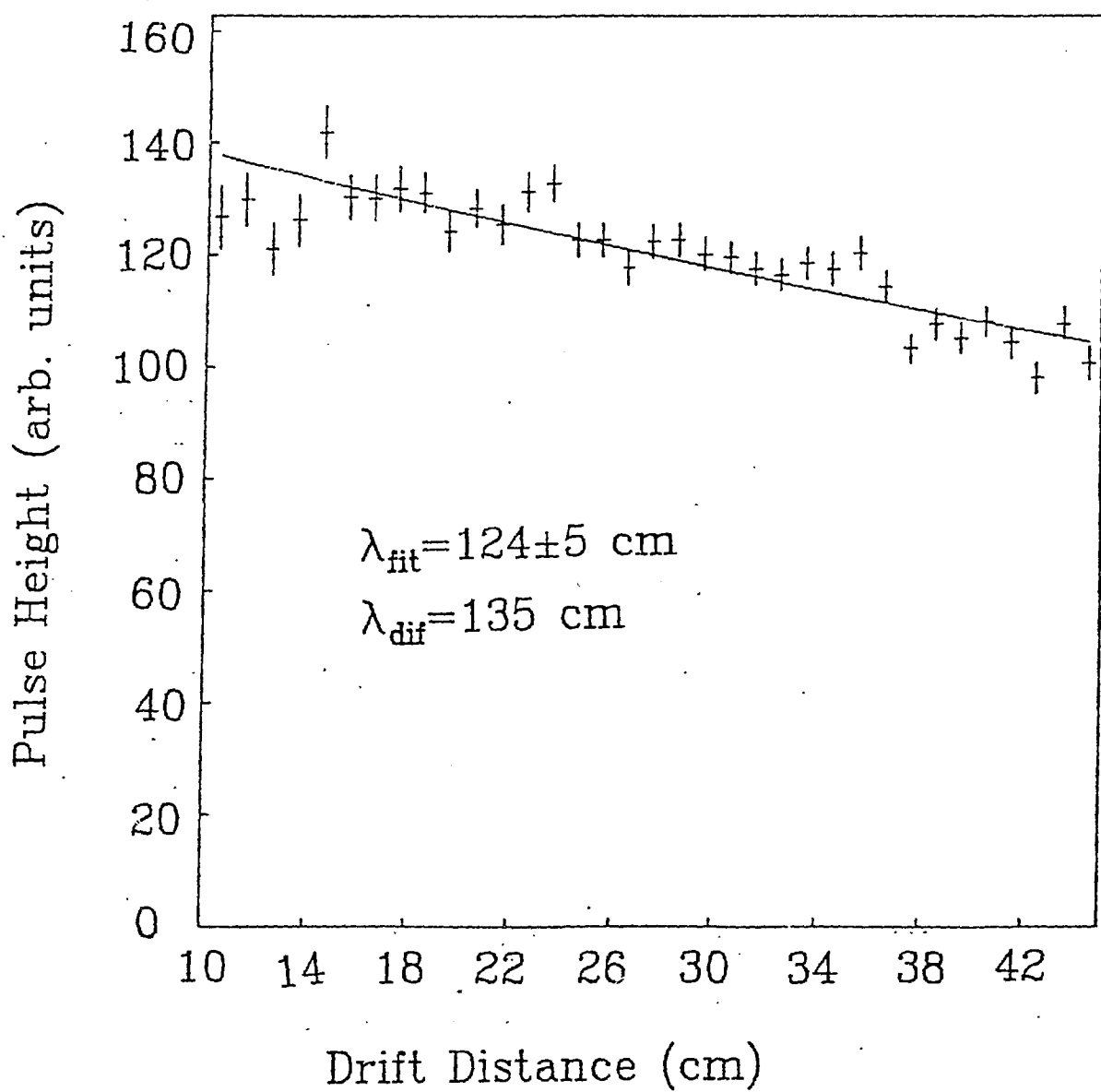


Fig. 6. An attenuation plot of pulse height versus drift distance.

Ionization Rise Measured from Stopping Muons

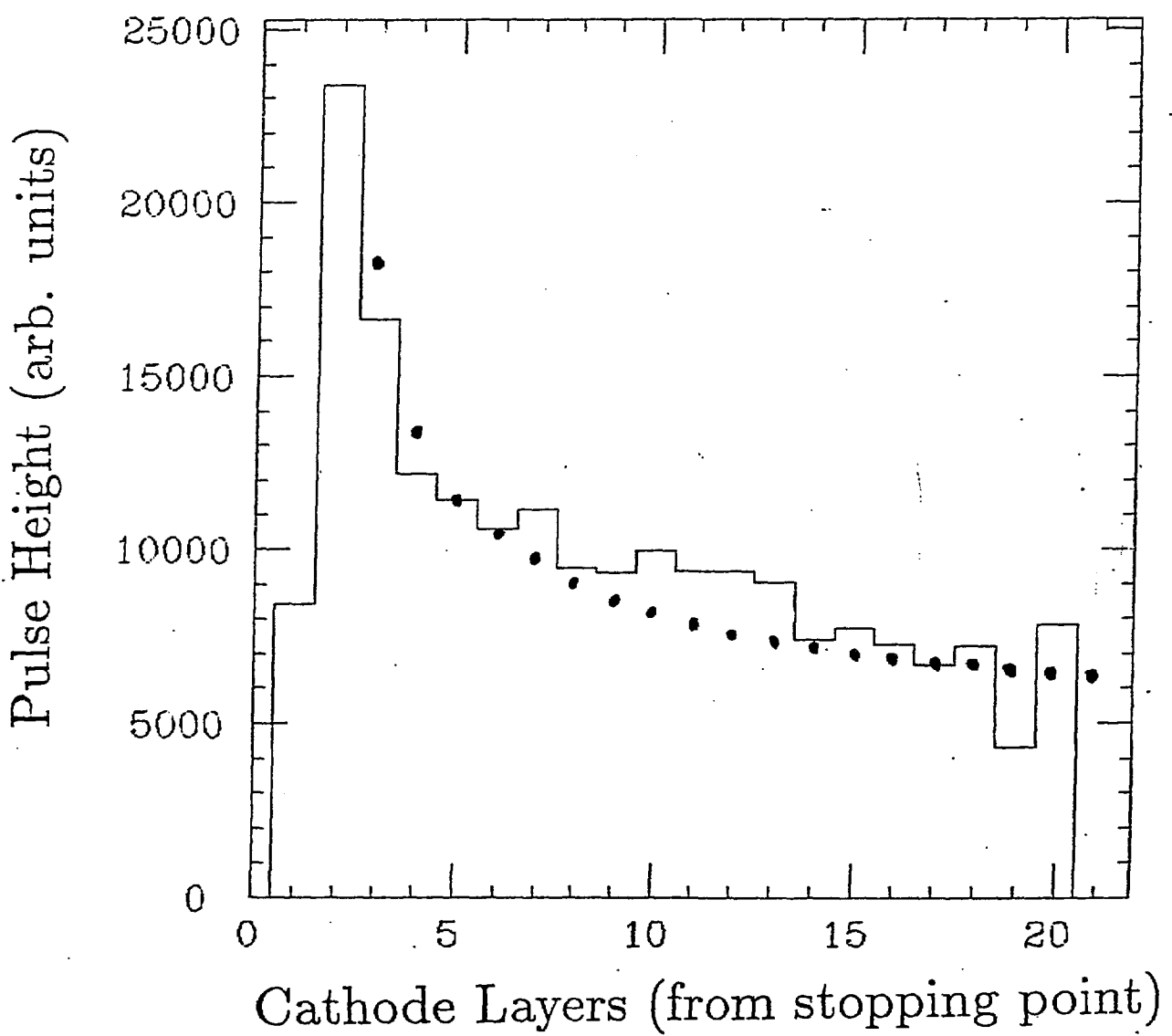


Fig. 7. The ionization rise from stopping muons as they approach their end point. The superposed points are the Bethe-Bloch equation.

Track Direction Determination for Stopping Muons from Ionization Measurements.

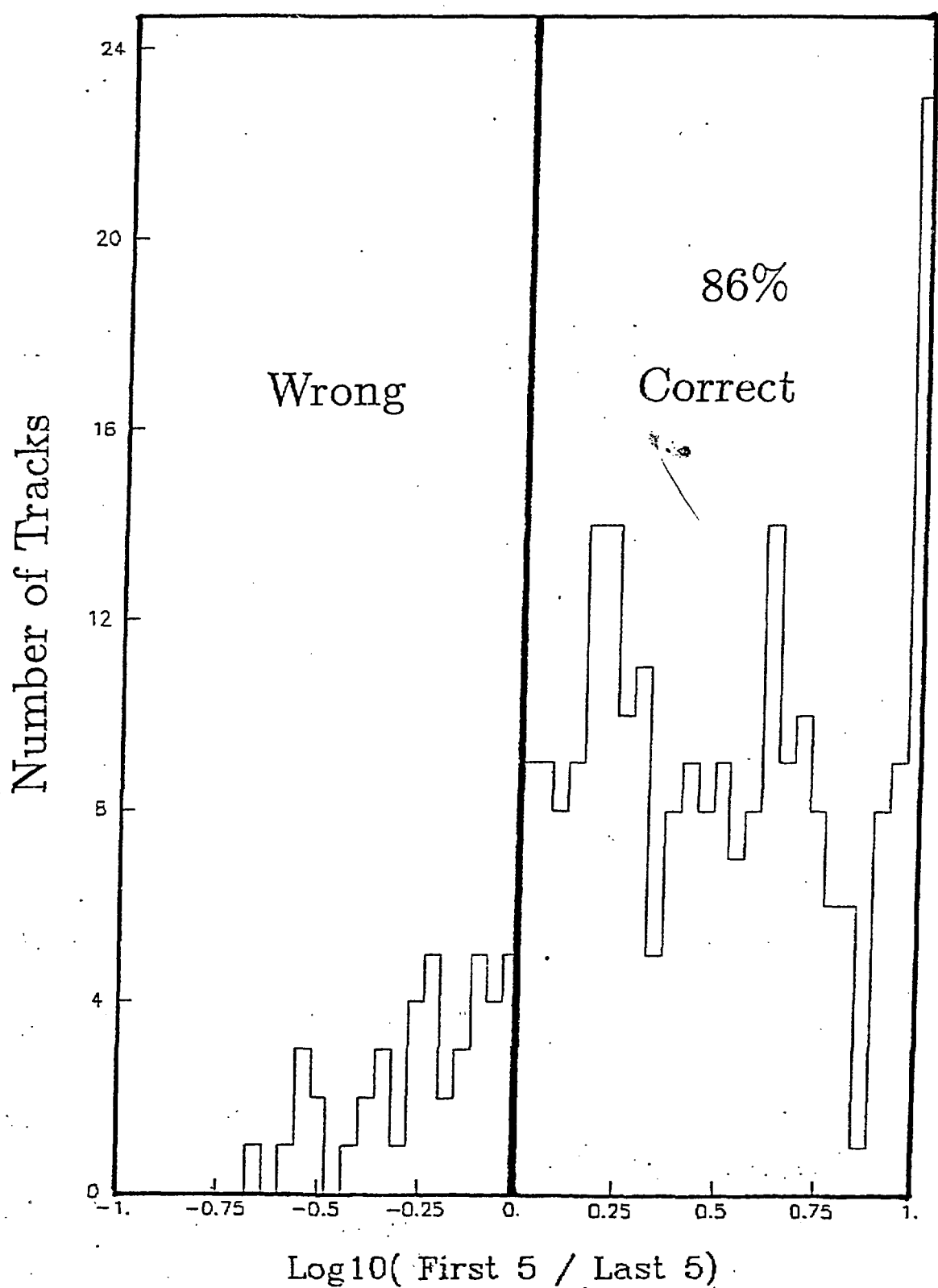


Fig. 8. Track direction determination for stopping muons on a track by track basis.